Supplement of Hydrol. Earth Syst. Sci., 30, 5297–5325, 2026
https://doi.org/10.5194/hess-30-5297-2026-supplement

Hydrology and Earth System Sciences
Open Access

Supplement of

Lake Victoria to the Sudd Wetland: flood wave timing, connectivity and wetland buffering across the White Nile

Douglas Mulangwa et al.

Correspondence to: Douglas Mulangwa (d.mulangwa@pgr.reading.ac.uk)

Supplementary

S.1 Sub-catchment Delineation, Hydrological Connectivity, and Geomorphological Setting

Catchment boundaries were delineated using HydroSHEDS level 4-6 sub-basins (Lehner and Grill, 2013) and cross-referenced against national hydrological planning frameworks to ensure alignment with management-relevant units. Specifically, Uganda's Water Management Zones (MWE, 2009) and South Sudan's Irrigation Development Master Plan (MEDIWR, 2015) were used to validate and refine sub-catchment definitions, particularly where sub-national boundaries influence rainfall aggregation and flood response assessment. These delineations enabled spatial aggregation of rainfall and flood-response data within hydrologically coherent upstream-downstream units. The spatial arrangement of the delineated sub-catchments, major lakes and rivers, Sudd Wetland extent, and key observation stations is presented in Fig. 1 of the main manuscript.

Sub-catchments 2-6 drain into Lake Victoria (sub-catchment 1), which was treated as a standalone sub-catchment because of its dominant upstream role and substantial direct rainfall contribution. Outflows from Lake Victoria at Jinja are regulated under the Agreed Curve (Kull, 2006) before draining northwards into Lake Kyoga (sub-catchment 7), which receives both upstream inflow and local rainfall contributions. Lake Kyoga subsequently drains into Lake Albert together with additional direct rainfall inputs from sub-catchments 8 and 9.

The Lake Kyoga basin contains extensive swamp and wetland systems surrounding the main lake and its satellite water bodies, including approximately 4,510 km² of swamp adjacent to about 1,760 km² of open water (Brown and Sutcliffe, 2013). These wetlands are largely dominated by papyrus and aquatic vegetation (Ma et al., 2024; NEMA, 2008) and contribute substantially to flood attenuation and delayed downstream routing. The Victoria, Kyoga, and Albert basins were therefore analysed as distinct hydrological units with differing tributary inflows and internal storage dynamics.

Further downstream, sub-catchments 10-15 generate rainfall-driven inflows into the Sudd Wetland through tributaries approaching from multiple directions. The main Nile channel traverses the Bahr el Jebel sub-catchment before entering the Sudd Wetland.

The Sudd lies within a broad paleo-lake depression frequently interpreted as the remnant of a former "Mega-lake Sudd" (Álvarez, 2023; Sutcliffe and Parks, 1999). This geomorphological setting reflects earlier drainage reorganisations, including Neogene reversals during which parts of the upper Nile basin drained westward toward the Congo Basin before capture into the present northward-flowing Nile system (Abdelsalam, 2018; Holzförster and Schmidt, 2007; Issawi and Farouk, 2023; Stankiewicz and de Wit, 2006).

The paleo-lake topography surrounding the Sudd promotes activation of braided wetland water pathways, facilitating lateral water movement and backwater interactions between adjacent sub-catchments (Mertes, 1997; Sutcliffe and Parks, 1999). Consequently, although the Sudd-connected sub-catchments were treated as indicative hydrological units, the wetland's hydrology departs from classical catchment behaviour. During prolonged high-flow periods, widespread wetland activation facilitates lateral spillovers across nominal sub-catchment boundaries and promotes complex floodplain connectivity.

S.2 Rainfall Anomalies, Lake Response, and Inter-Lake Timing

S2.1 SPI-6 Methodology

Rainfall anomalies were analysed to characterise basin-scale meteorological forcing and to provide context for the flood-wave propagation analysed in Sect. 2.4. Daily precipitation anomalies were quantified using the Standardized Precipitation Index (SPI) (Guttman, 1999) computed at a 180-day accumulation window (SPI-6). SPI-6 was selected instead of shorter accumulation windows (e.g. SPI-3) to capture the long hydrological memory characteristic of the White Nile system, where rainfall signals can propagate through the series of lakes and wetlands over several months to more than a year (Sutcliffe and Parks, 1999; Williams, 2018).

Daily resolution was used while retaining multi-month memory too by forming rolling 180-day accumulations of daily rainfall. For each catchment i and day t, the rolling sum was computed as:

$$S_{180,i}(t) = \sum_{k=0}^{179} P_i(t-k)$$

Where $P_i(t)$ is daily precipitation. To avoid unstable values near gaps, a sum was only taken when at least 90 % of the days in the window were available. This ensured stable estimation of accumulated rainfall while guarding against any artefacts in the data.

A fixed baseline of 1983–2017 was adopted, spanning the mature satellite era for CHIRPS (Funk et al., 2015) and preceding the recent high-lake period under study. To account for seasonality, each calendar day t was matched to a ±15-day pool by day-of-year within the baseline. For example, an SPI-6 value on 10 June is compared against all baseline S180 values falling between 26th May and 25th June. This approach preserves seasonal comparability while maintaining sufficient sample size (31 days × 35 years = 1,085 observations per pool).

Within each day-of-year pool, the accumulated rainfall values were fitted to a two-parameter gamma distribution, following the standard SPI procedure. Percentiles were obtained from this fitted distribution and converted to standard normal deviates using the inverse Gaussian transformation (Guttman, 1999). This parametric approach preserves the conventional interpretation of SPI as a normally distributed index of wetness or dryness. SPI-6 time series were computed per contributing sub-catchment.

Anomalies were visualised using continuous daily SPI-6 heatmaps to highlight temporal persistence and seasonality of wet and dry phases. A diverging colour palette (wet = blue, dry = red) was applied, with reference bands indicating standard SPI categories: severely wet (SPI

≥ 2.0), moderately wet (1.0 ≤ SPI < 2.0), near-normal (−1.0 < SPI < 1.0), moderately dry (−2.0 < SPI ≤ −1.0), and severely dry (SPI ≤ −2.0). These categories are provided as interpretive guides rather than formal thresholds (Guttman, 1999).

To provide meteorological context for the tracked flood-wave events, CHIRPS rainfall was additionally aggregated as rolling 180-day totals, consistent with both the SPI-6 accumulation window and the long hydrological memory characteristic of the White Nile system (Funk et al., 2015). Daily precipitation values were first spatially aggregated to catchment-scale means for each analysis unit or lake, and where multiple contributing sub-catchments were present, area-weighted averages were applied. These rolling rainfall accumulations were plotted alongside the flood-wave time series using secondary axes to facilitate visual comparison between rainfall forcing and downstream hydrological response.

Rainfall on these plots was included for interpretive context only and was not used for quantitative lag estimation. The objective was to compare the timing and persistence of rainfall inputs relative to observed flood-wave propagation and storage responses across the lake-river-wetland system. This interpretive framework follows earlier studies examining precipitation-hydrology phase relationships across the White Nile Basin (Mistry and Conway, 2003; Nicholson et al., 2021; Vanderkelen et al., 2018a, b; Yin and Nicholson, 2002).

S2.2 Seasonal Rainfall Anomalies and Lake Response

SPI-6 anomalies reveal a coherent multi-season pluvial episode that developed across much of the Upper White Nile basin beginning in late 2019 (*Figs. S1 and S2*). The wet phase was characterised by four successive anomalous rainy seasons spanning OND 2019, MAM 2020, OND 2020, and MAM 2021, during which positive rainfall anomalies developed near-simultaneously across multiple sub-catchments and persisted through successive seasonal cycles with limited intervening recession. The timing and spatial extent of these anomalies coincide with the extreme positive Indian Ocean Dipole (IOD) event of 2019, which intensified short-rains convection across East Africa (Ratna et al., 2021; Ummenhofer et al., 2009; Wainwright et al., 2021; Zhang et al., 2021).

The strongest and most persistent wet anomalies occurred within the Lake Victoria contributing catchments (Lake Victoria, Kagera, Mara-Nyando, Nzoia-Sio, Katonga, and Isanga-Simiyu), sustaining inflows and directly contributing to the exceptional rise and prolonged high levels observed across the downstream lake-river cascade (*Fig. S1*). Within the Kyoga basin, rainfall remained above average into early 2021, producing extended wet-season recharge that maintained elevated lake and wetland levels through 2022 before recession began during 2023. In contrast, the Albert basin exhibited only moderate local wet anomalies, suggesting that sustained high lake levels were driven primarily by upstream inflows transmitted through the Victoria-Kyoga system rather than by local rainfall forcing alone.

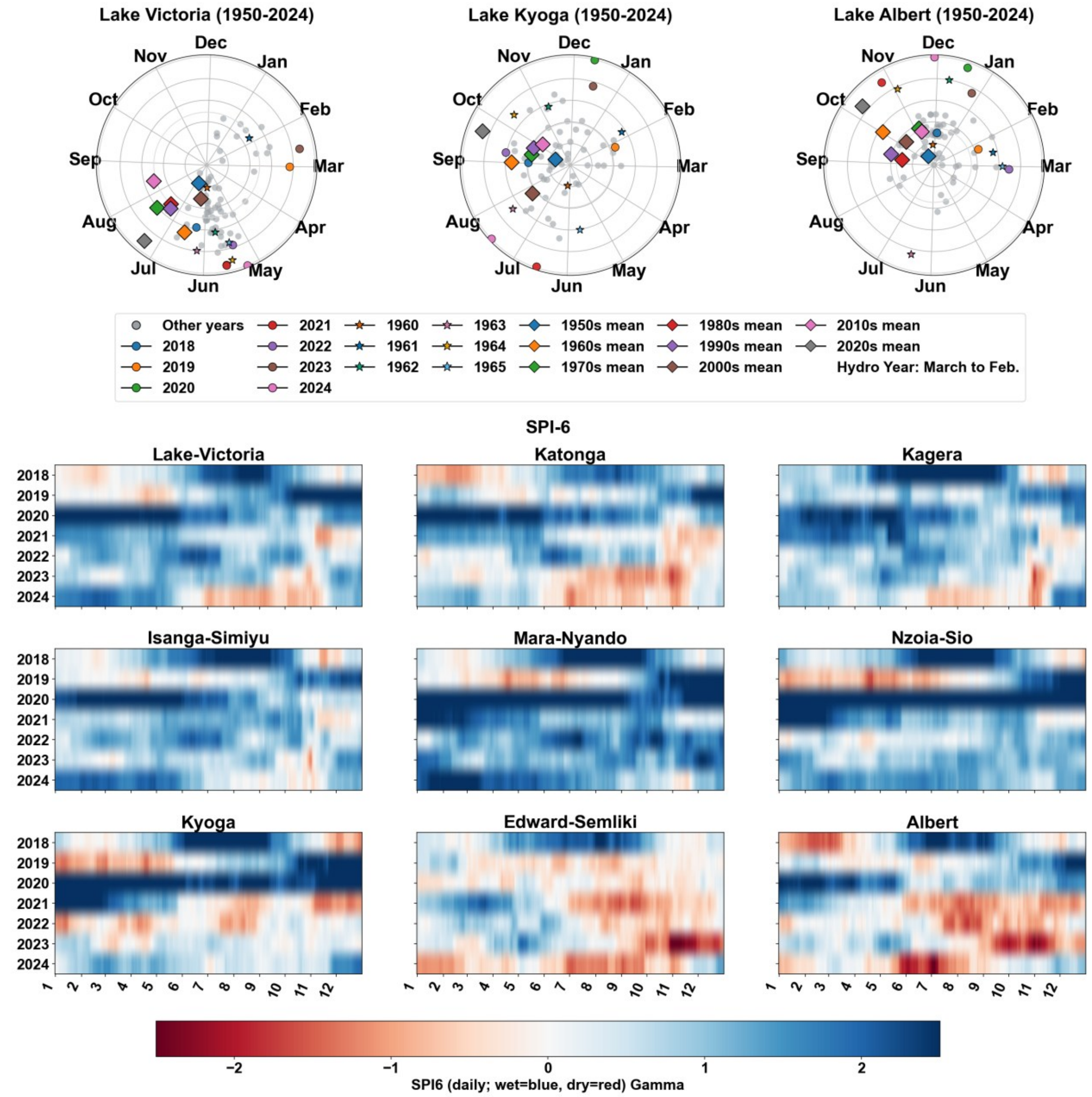

Fig. S1.: Seasonality of annual maxima (top panels) and rainfall anomalies (bottom panels) for the main lake basins. The top panels show the timing of annual maxima for Lakes Victoria, Kyoga, and Albert during 1950-2024, grouped by decade and referenced to the hydrological year (March–February). The lower panels present six-month Standardized Precipitation Index (SPI-6) anomalies for 2018–2024 relative to the 1983–2017 climatology. The palette (wet = blue, dry = red) follows standard SPI categories: severely wet (SPI ≥ 2.0), moderately wet (1.0 ≤ SPI < 2.0), near-normal (−1.0 < SPI < 1.0), moderately dry (−2.0 < SPI ≤ −1.0), and severely dry (SPI ≤ −2.0). Catchments contributing to each lake are grouped as follows: Katonga, Kagera, Isanga-Simiyu, Mara-Nyando, and Nzoia-Sio drain into Lake Victoria; Kyoga drains into Lake Kyoga; and Edward-Semliki and Albert drain into Lake Albert.

Downstream, the Sudd-feeding sub-catchments displayed greater spatial heterogeneity (*Fig. S2*). Baro-Akobbo-Sobat and the eastern White Nile broadly mirrored the 2019-2020 wet phase, whereas Bahr el Jebel and Bahr el Ghazal alternated between wet and near-normal conditions, reflecting their transitional hydroclimatic position between equatorial and Sudano-Sahelian rainfall regimes (Nicholson, 2017; Sutcliffe and Parks, 1999).

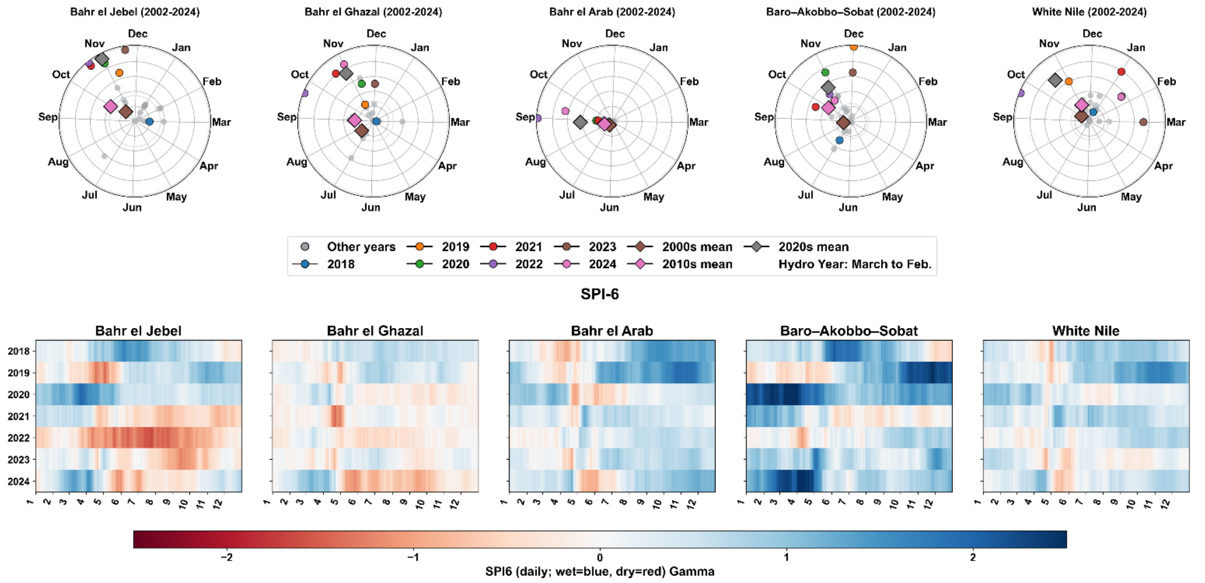

Fig. S2: Seasonality of annual maxima (top panels) and rainfall anomalies (bottom panels) for the South Sudan sub-catchments based on MODIS wetland extent and SPI-6 rainfall indices. The top panels show the timing of annual wetland-extent maxima for Bahr el Jebel, Bahr el Ghazal, Bahr el Arab, Baro Akobbo Sobat, and the White Nile during 2002-2024, grouped by decade and referenced to the hydrological year (March–February). The lower panels present six-month Standardized Precipitation Index (SPI-6) anomalies for 2018–2024 relative to the 1983–2017 climatology. The palette (wet = blue, dry = red) follows standard SPI categories: severely wet (SPI ≥ 2.0), moderately wet (1.0 ≤ SPI < 2.0), near-normal (−1.0 < SPI < 1.0), moderately dry (−2.0 < SPI ≤ −1.0), and severely dry (SPI ≤ −2.0).

Taken together, these spatially extensive and persistent SPI-6 anomalies explain the sustained high lake levels observed during 2019-2022, highlighting the basin-wide influence of the 2019 IOD-driven rainfall anomaly. The wet phase was characterised by four successive anomalous rainy seasons spanning OND 2019, MAM 2020, OND 2020, and MAM 2021, which maintained persistently elevated hydrological inputs across much of the Upper White Nile basin. However, rainfall anomalies weakened or became more spatially heterogeneous across several upstream basins after 2021 (*Fig. S1*), whereas downstream wetland inundation and elevated flood responses persisted through 2022 within parts of the Sudd system (*Fig. S2*). This divergence between declining rainfall anomalies and continued downstream flooding indicates that multi-year storage and delayed release within the lake-river-wetland system played a central role in sustaining inundation.

S2.3 Annual Maxima and Inter-Lake Timing

Across 1950-2024, annual maxima followed a clear downstream progression, with Lake Victoria peaking on average on 10 May (n=75), Lake Kyoga on 28 September (n=62), and Lake Albert on 9 December (n=71) (*Fig. S1*). This sequence reflects both latitudinal rainfall phasing and cumulative storage effects, with flood waves progressively delayed and attenuated along the Victoria-Kyoga-Albert cascade through successive lakes and wetlands (Nicholson, 2017; Sutcliffe and Parks, 1999).

Decadal analysis indicates that while long-term mean timing remained relatively stable, inter-decadal variability was substantial. Lake Victoria peaks were concentrated between mid-May and early June from the 1950s through the 2000s but shifted markedly earlier during the 2010s (mean: 24 March). Lake Kyoga peaks generally clustered between September and December, except for unusually late behaviour during the 2000s (16 December) and earlier peaks during the 1980s (7 September). Lake Albert exhibited the broadest spread in timing, with peaks ranging from mid-October during the 1980s to late January during the 1990s before stabilising closer to December during the 2000s and 2010s.

During the 2018-2024 high-water period, peak timing diverged substantially from the historical pattern. In Lake Victoria, some annual maxima occurred much earlier than the long-term mean, notably on 29 February 2019 and 18 February 2023, both preceding the historical average by nearly three months. Between 2020 and 2022, lake levels remained persistently elevated with limited evidence of seasonal recession, indicating prolonged storage following the successive anomalous wet seasons of 2019-2021 (Wainwright et al., 2021) (*Fig. S1*).

Lake Kyoga displayed pronounced irregularity, with annual peaks spanning nearly the full hydrological year from February 2019 to July 2024 (*Fig. S1*). This disrupted sequence included exceptionally high stages during 2021 and 2022, when routing through the Kyoga wetland complex slowed substantially and floodplain inundation persisted across successive seasons. Such behaviour reflects the basin's strong buffering capacity and slow drainage response, consistent with previous observations of sustained wetland inundation and delayed outflow toward Lake Albert (Brown and Sutcliffe, 2013; Ma et al., 2024; NEMA, 2008).

Lake Albert followed a similar pattern, maintaining elevated base levels through 2021 and 2022 despite relatively modest local rainfall anomalies. Peaks in December 2020 and March 2022 (*Fig. S1*), both unusually high, indicate that sustained inflows from Victoria and Kyoga maintained saturated conditions across the downstream lake-river system for several consecutive years. This persistence highlights the multi-year hydrological memory of the lake-river cascade and preceded the widespread wetland expansion observed within the Sudd system during 2021-2022 (*Fig. S2*).

Beyond Lake Albert, the flood signal propagated into the South Sudan sub-catchments, where exceptionally low relief and paleo-lake topography promoted broad wetland expansion and lateral hydrological connectivity (Álvarez, 2023; Mertes, 1997; Sutcliffe and Parks, 1999). Bahr el Jebel, positioned immediately downstream of Lake Albert, exhibited the earliest and strongest responses, with flood extents rising sharply during 2020-2022 in step with sustained upstream inflow. Elevated stages along Bahr el Jebel raised the hydraulic base level of the Sudd, facilitating spillover into adjacent zones such as Bahr el Ghazal and Bahr el Arab. Bahr el Ghazal showed delayed and dampened peaks, consistent with secondary activation through lateral inflow and backwater influence rather than direct channel transmission. Bahr el Arab displayed a more intermittent pattern dominated by local rainfall but experienced pronounced wetland activation during 2022 when exceptionally high Bahr el Jebel levels extended the inundation footprint northwestward.

On the eastern side, Baro-Akobbo-Sobat responded more strongly to regional rainfall over the Ethiopian Highlands and, to some extent, to spillover from Bahr el Jebel and the White Nile sub-catchments, indicating compound hydrological influence rather than a purely upstream-driven flood wave. The White Nile corridor itself remained persistently wet during 2020-2022, with subdued hydrograph behaviour reflecting integrated storage within the Sudd and downstream backwater influence near Malakal. Such prolonged wetland persistence and spatial coherence are consistent with earlier observations linking sustained Sudd inundation to elevated equatorial lake inflows and delayed wetland release (Mohamed et al., 2005a, b; Mohamed and Savenije, 2014; Nicholson, 2017; Sutcliffe and Parks, 1999), as well as more recent studies documenting persistent wetland connectivity following the 2019 positive IOD event (Hardy et al., 2023; Pietroiusti et al., 2024; Wainwright et al., 2021).

Taken together, the disruption in the timing and duration of annual maxima during 2019-2024 indicates that the event represented not only a rainfall anomaly but also a substantial shift in flood-wave translation and storage behaviour across the lake-river-wetland system. These timing anomalies and prolonged wetland responses provide supporting evidence for the delayed downstream propagation and extended transit times analysed in the main manuscript.

S.3 Sensitivity Analysis of Event-Matching Parameters

To evaluate the robustness of inferred Lake Victoria-to-Sudd flood-wave transit times to key event-matching parameters, a supplementary sensitivity analysis was conducted. Sensitivity analysis is commonly used to assess the stability of model-derived outcomes to parameter selection and methodological assumptions (Pianosi et al., 2016; Saltelli et al., 2010). Using the flood-wave tracking framework described in Sect. 2.4, the analysis assessed the influence of smoothing-window length and downstream search-horizon constraints on the derived system-scale transit times.

A grid-based one-at-a-time (OAT) sensitivity analysis was performed in which the smoothing window applied to the hydrographs was varied from 1 to 90 days and the downstream segment search horizon from 20 days to approximately 3 years, while all other components of the event-matching framework were held fixed. These included the sequential forward-routing structure, fixed 31-day event windows, chronology constraints, and the prominence threshold (δ) used in the baseline analysis. The tested parameter space encompassed both shorter smoothing windows, including a 7-day window, and substantially broader search-horizon ranges designed to evaluate the stability of the inferred transit-time signal.

The resulting sensitivity surfaces indicate that inferred system transit times are largely insensitive to smoothing-window choice across the tested range, with only minor variability introduced by increased smoothing length (*Fig. S3*). In contrast, the downstream search horizon exerted the dominant control on resultant lag estimates. For search horizons up to approximately 1.25 years, the tested parameter combinations consistently produced system transit times clustered around ~15-17 months, supporting the mean Lake Victoria-to-Sudd transit time reported in the main manuscript.

For substantially longer search horizons, the algorithm increasingly matched Lake Victoria flood-wave events with later Sudd wetland expansions that were unlikely to be causally connected to the originating upstream signal. This produced artificially extended lag estimates and multimodal lag distributions, as illustrated by the grouped violin plots in *Fig. S3*. These longer-lag solutions primarily emerged when the search horizon exceeded physically plausible routing and storage timescales for the observed flood-wave propagation sequence.

Overall, the sensitivity analysis demonstrates that the reported mean system transit time of approximately 17 months (16.84±1.95 months) represents a robust hydrological signal rather than an artefact of subjective parameter selection. The relative insensitivity to smoothing-window choice, combined with the physically interpretable behaviour of the search-horizon constraint, provides additional confidence that the inferred transit times reflect genuine storage-mediated downstream propagation across the White Nile lake-river-wetland system.

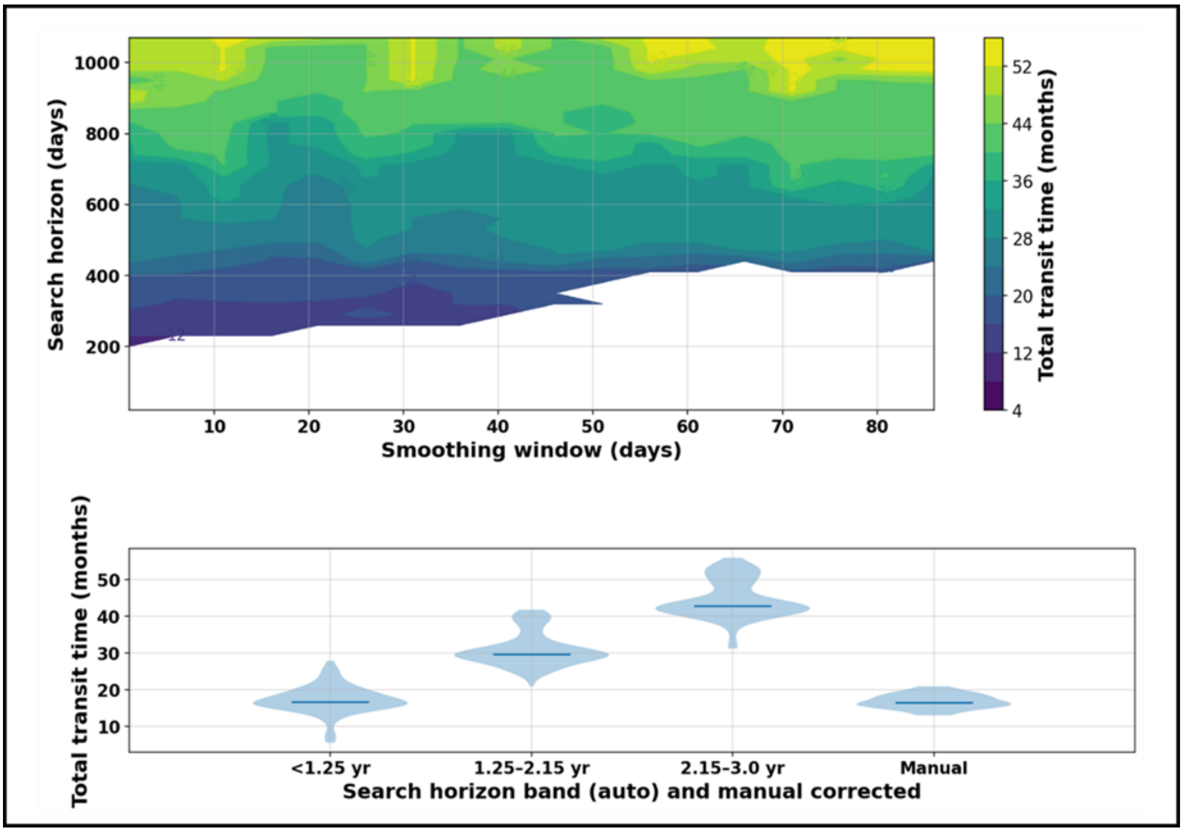

Fig. S3: Sensitivity analysis of inferred Lake Victoria-to-Sudd system transit times to key event-matching parameters. The upper panel shows the contour response of total transit time to variations in smoothing-window length and downstream search horizon. The lower panel shows violin distributions of inferred transit times grouped by search-horizon range, alongside the manually corrected estimates used in the main analysis.

References

Abdelsalam, M. G.: The Nile's journey through space and time: A geological perspective, https://doi.org/10.1016/j.earscirev.2018.01.010, 1 February 2018., 2018.

Álvarez, W.: An enormous Pliocene or Quaternary Megalake Sudd on the River Nile in the Sudan Basin? A review of the dilemma, and a possible solution, https://doi.org/10.1016/j.jafrearsci.2023.105016, 1 December 2023., 2023.

Brown, E. and Sutcliffe, J. V.: The water balance of Lake Kyoga, Uganda, Hydrological Sciences Journal, 58, 342–353, https://doi.org/10.1080/02626667.2012.753148, 2013.

Funk, C., Peterson, P., Landsfeld, M., Pedreros, D., Verdin, J., Shukla, S., Husak, G., Rowland, J., Harrison, L., Hoell, A., and Michaelsen, J.: The climate hazards infrared precipitation with stations - A new environmental record for monitoring extremes, Sci. Data, 2, https://doi.org/10.1038/SDATA.2015.66, 2015.

Guttman, N. B.: Accepting the standardized precipitation index: A calculation algorithm, J. Am. Water Resour. Assoc., 35, 311–322, https://doi.org/10.1111/j.1752-1688.1999.tb03592.x, 1999.

Hardy, A., Palmer, P. I., and Oakes, G.: Satellite data reveal how Sudd wetland dynamics are linked with globally-significant methane emissions, Environmental Research Letters, 18, https://doi.org/10.1088/1748-9326/ace272, 2023.

Holzförster, F. and Schmidt, U.: Anatomy of a river drainage reversal in the Neogene Kivu-Nile Rift, Quat. Sci. Rev., 26, 1771–1789, https://doi.org/10.1016/j.quascirev.2007.04.018, 2007.

Issawi, B. and Farouk, S.: Evolution of the Nile River Through Time, in: Advances in Science, Technology and Innovation, Springer Nature, 491–498, https://doi.org/10.1007/978-3-030-95637-0_17, 2023.

Kull, D.: Connections Between Recent Water Level Drops in Lake Victoria, Dam Operations and Drought, 2006.

Lehner, B. and Grill, G.: Global river hydrography and network routing: Baseline data and new approaches to study the world's large river systems, Hydrol. Process., 27, 2171–2186, https://doi.org/10.1002/HYP.9740, 2013.

Ma, Y., Gopal, S., Koch, M., and Kaufman, L.: Mapping the dynamics of aquatic vegetation in Lake Kyoga and its linkages to satellite lakes, Science of Remote Sensing, 10, https://doi.org/10.1016/j.srs.2024.100156, 2024.

MEDIWR: Irrigation Development Master Plan (IDMP) In The Republic of South Sudan, 2015.

Mertes, L. A. K.: Documentation and significance of the perirheic zone on inundated floodplains, Water Resour. Res., 33, 1749–1762, https://doi.org/10.1029/97WR00658, 1997.

Mistry, V. V. and Conway, D.: Remote forcing of east African rainfall and relationships with fluctuations in levels of lake Victoria, International Journal of Climatology, 23, 67–89, https://doi.org/10.1002/joc.861, 2003.

Mohamed, Y. A. and Savenije, H. H. G.: Impact of climate variability on the hydrology of the Sudd wetland: Signals derived from long term (1900-2000) water balance computations, Wetl. Ecol. Manag., 22, 191–198, https://doi.org/10.1007/S11273-014-9337-7/FIGURES/5, 2014.

Mohamed, Y. A., Van Den Hurk, B. J. J. M., Savenije, H. H. G., and Bastiaanssen, W. G. M.: Hydroclimatology of the Nile: results from a regional climate model, Hydrology and Earth System Sciences, 263–278 pp., https://doi.org/10.5194/hess-9-263-2005, 2005a.

Mohamed, Y. A., Van Den Hurk, B. J. J. M., Savenije, H. H. G., and Bastiaanssen, W. G. M.: Impact of the Sudd wetland on the Nile hydroclimatology, Water Resour. Res., 41, 1–14, https://doi.org/10.1029/2004WR003792, 2005b.

MWE: WATER MANAGEMENT ZONES (WMZ) | Ministry of Water and Environment, https://www.mwe.go.ug/library/water-management-zones-wmz, last access: 14 June 2024, 2009., 2009.

NEMA: Pilot Integrated Ecosystem Assessment of the Lake Kyoga Catchment Area, http://www.nemaug.org, 2008.

Nicholson, S. E.: Climate and climatic variability of rainfall over eastern Africa, Reviews of Geophysics, 55, 590–635, https://doi.org/10.1002/2016RG000544, 2017.

Nicholson, S. E., Klotter, D., and Hartman, A. T.: Lake-effect rains over lake victoria and their association with mesoscale convective systems, J. Hydrometeorol., 22, 1353–1368, https://doi.org/10.1175/JHM-D-20-0244.1, 2021.

Pianosi, F., Beven, K., Freer, J., Hall, J. W., Rougier, J., Stephenson, D. B., and Wagener, T.: Sensitivity analysis of environmental models: A systematic review with practical workflow, https://doi.org/10.1016/j.envsoft.2016.02.008, 1 May 2016., 2016.

Pietroiusti, R., Vanderkelen, I., Otto, F. E. L., Barnes, C., Temple, L., Akurut, M., Bally, P., Van Lipzig, N. P. M., and Thiery, W.: Possible role of anthropogenic climate change in the record-breaking 2020 Lake Victoria levels and floods, Earth System Dynamics, 15, 225–264, https://doi.org/10.5194/esd-15-225-2024, 2024.

Ratna, S. B., Cherchi, A., Osborn, T. J., Joshi, M., and Uppara, U.: The Extreme Positive Indian Ocean Dipole of 2019 and Associated Indian Summer Monsoon Rainfall Response, Geophys. Res. Lett., 48, https://doi.org/10.1029/2020GL091497, 2021.

Saltelli, A., Annoni, P., Azzini, I., Campolongo, F., Ratto, M., and Tarantola, S.: Variance based sensitivity analysis of model output. Design and estimator for the total sensitivity index, Comput. Phys. Commun., 181, 259–270, https://doi.org/10.1016/j.cpc.2009.09.018, 2010.

Stankiewicz, J. and de Wit, M. J.: A proposed drainage evolution model for Central Africa - Did the Congo flow east?, Journal of African Earth Sciences, 44, 75–84, https://doi.org/10.1016/j.jafrearsci.2005.11.008, 2006.

Sutcliffe, J. V and Parks, Y. P.: The Hydrology of the Nile, 1999.

Ummenhofer, C. C., Gupta, A. Sen, England, M. H., and Reason, C. J. C.: Contributions of Indian Ocean sea surface temperatures to enhanced East African rainfall, J. Clim., 22, 993–1013, https://doi.org/10.1175/2008JCLI2493.1, 2009.

Vanderkelen, I., Van Lipzig, N. P. M., and Thiery, W.: Modelling the water balance of Lake Victoria (East Africa)-Part 1: Observational analysis, Hydrol. Earth Syst. Sci., 22, 5509–5525, https://doi.org/10.5194/hess-22-5509-2018, 2018a.

Vanderkelen, I., Van Lipzig, N. P. M., and Thiery, W.: Modelling the water balance of Lake Victoria (East Africa)-Part 2: Future projections, Hydrol. Earth Syst. Sci., 22, 5527–5549, https://doi.org/10.5194/hess-22-5527-2018, 2018b.

Wainwright, C. M., Finney, D. L., Kilavi, M., Black, E., and Marsham, J. H.: Extreme rainfall in East Africa, October 2019–January 2020 and context under future climate change, Weather, 76, 26–31, https://doi.org/10.1002/WEA.3824, 2021.

Williams, M.: The Sudd Swamps and the White Nile, in: The Nile Basin, Cambridge University Press, 107–126, https://doi.org/10.1017/9781316831885.009, 2018.

Yin, X. and Nicholson, S. E.: Interpreting Annual Rainfall from the Levels of Lake Victoria, 2002.

Zhang, L. and Han, W.: Interbasin and Multiple-Time-Scale Interactions in Generating the 2019 Extreme Indian Ocean Dipole, https://doi.org/10.1175/JCLI-D-20, 2021.